Dwarf Galaxies: From the Deep Universe to the Present
Proceedings IAU Symposium No. 344, 2019
K. B. W. McQuinn & S. Stierwalt, eds.

doi:10.1017/S1743921318006233

The evolution of the luminosity function faint end of cluster galaxies in the Cluster-EAGLE simulation

Andrea Negri[1,2], Claudio Dalla Vecchia[1,2], Alfonso Aguerri[1,2], Yannick Bahé[3,4], David Barnes[5,6] and Scott Kay[6]

[1]Instituto de Astrofísica de Canarias, C/Vía Lactea s/n, E-38205 La Laguna, Tenerife, Spain
email: anegri@iac.es

[2]Departamento de Astrofísica, Universidad de La Laguna, Av. del Astrofísico Francisco Sanchez s/n, E-38205 La Laguna, Tenerife, Spain

[3]Leiden Observatory, Leiden University, PO Box 9513, NL-2300 RA Leiden, the Netherlands

[4]Max-Planck-Institut fur Astrophysik, Karl-Schwarzschild Str. 1, D-85748 Garching, Germany

[5]Department of Physics, Kavli Institute for Astrophysics and Space Research, Massachusetts Institute of Technology, Cambridge, MA 02139, USA

[6]Jodrell Bank Centre for Astrophysics, School of Physics and Astronomy, The University of Manchester, Manchester M13 9PL, UK

Abstract. In the last decade observations have been able to probe the evolution of the galaxy luminosity function, in particular showing a variation of its faint-end with redshift. We employ the data of the Cluster-EAGLE project, a set of cosmological, hydrodynamical zoom-in simulations of 30 galaxy clusters, to study the evolution of the galaxy luminostity functions in clusters with redshift. We compile a catalogue of simulated galaxies' luminosities in the SDSS bands using the E-MILES spectra database, and taking into account dust attenuation. Stacked luminosity functions present little evolution with redshift of the faint-end slope from z=3.5 to z=0, regardless of the cluster mass.

Keywords. galaxies: evolution, galaxies: formation, galaxies: dwarf, galaxies: high-redshif, methods: numerical

1. Introduction

The galaxy luminosity function (LF), which traces the number density of galaxies of a given luminosity, is a fundamental tool for exploring galaxy evolution over cosmic time. In the last decade observations have been able to probe the evolution of the galaxy LF with redshift, in particular showing a variation of its faint end (Blanton *et al.* 2005; Popesso *et al.* 2006; Barkhouse *et al.* 2007; Agulli *et al.* 2017, and references therein). Motivated by the lack of an extended numerical study of the evolution of the LF in clusters, we employed the Cluster-EAGLE simulation (Bahé *et al.* 2017; Barnes *et al.* 2017), a set of hydrodynamical cosmological zoom simulations of the formation of 30 galaxy clusters in the mass range $10^{14} < M_{200}/M_{\odot} < 10^{15.4}$, to probe the LF evolution during cosmic time.

2. Results

We compiled a catalogue of simulated galaxies' luminosities in the SDSS bands using the E-MILES spectra database (Vazdekis *et al.* 2016). We treated each stellar particle in the simulation (characterised by their initial mass, metallicity and age) as a single stellar population , and we derived their fluxes by convolving the synthetic spectra with

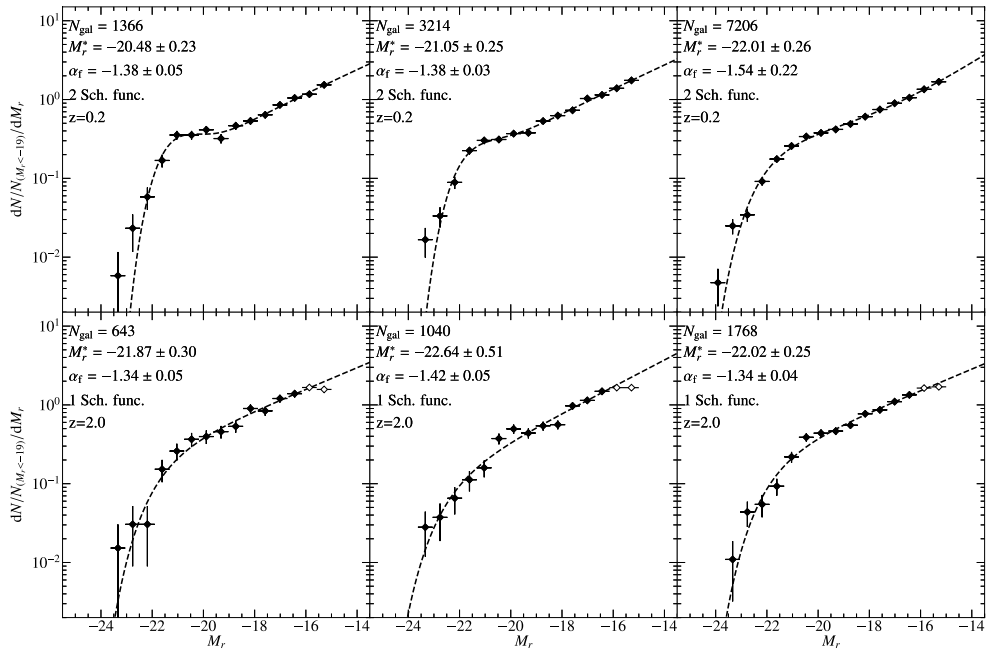

Figure 1. Stacked LFs for the 30 Cluster-EAGLE runs at two different redshifts (top and bottom rows). The cluster have been divided in 3 bins, having $\log(M_{200}) < 14.46$ (left column), $14.46 < \log(M_{200}/M_\odot) < 14.84$ (central column) and $\log(M_{200}/M_\odot) > 14.84$ (right column). Each LF is normalized at the number of galaxies having $M_r < -19$, while M_r^* and α_f denote the knee magnitude and the slope of the faint end, respectively. Empty circles (not considered in the fit) mark the magnitude bins affected by the finite resolution of the simulation.

the response of the SDSS passbands (u, g, r, i, z). Intrinsic dust attenuation has been computed following the standard modelling of Trayford *et al.* (2015), but normalizing the extinction law with the surface density of heavy elements in the gas phase, instead of their total mass. We found this prescription produces reasonable attenuation values over a wide range of stellar mass, and is compatible with the observational constraints of attenuation in massive ETGs. Recent (<100 Myr) star formation is resampled with finer time intervals, alleviating the effects of stochasticity of the star formation model. All spectra are computed within a three-dimensional aperture of 30 kpc.

In order to study the evolution in redshift of the luminosity function, we built 3 bins of M_{200} at $z = 0$, where each bin contains 10 clusters ordered by M_{200}. The members of the bins are then kept constant back in time, regardless of their M_{200} at different redshifts. We then selected the galaxies inside r_{200} for each cluster, removed the brightest galaxy from each group and stacked them by binning their r-band absolute magnitude M_r. We fit the resulting luminosity functions with with one and two Schechter functions, to take into account the upturn in the faint end, and the best fit is determined by the χ^2 test.

Figure 1 shows the stacked LFs at two different redshifts, for the three M_{200} bins, while Figure 2 presents the knee luminosity M_r^* and faint end slope α_f of the LF for the full sample, up to $z = 3.5$. Quite remarkably, the faint end slope does not evolve dramatically from high to low z, especially for intermediate-high mass clusters. Therefore, the faint end at high redshift is already in place at the centre of the protocluster, where the vast majority of high-z dwarfs are later merged (Negri *et al.*, in prep), while new faint galaxies falls in the cluster central region during its evolution.

https://doi.org/10.1017/S1743921318006233 Published online by Cambridge University Press

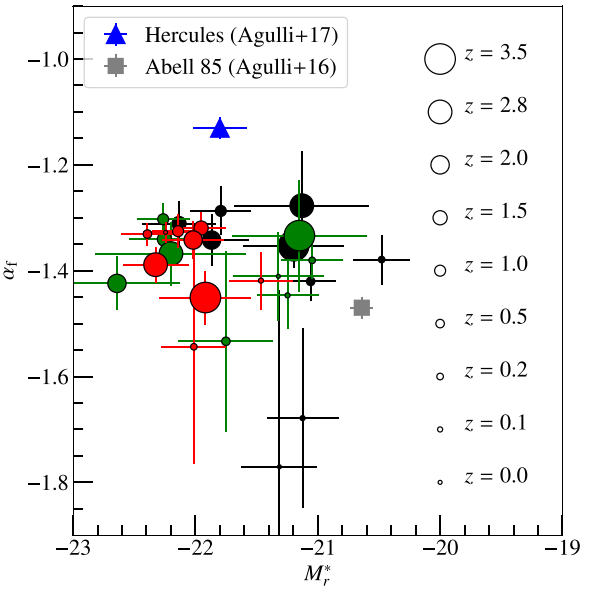

Figure 2. Knee luminosity M_r^* and faint end slope α_f of stacked LF for different redshifts (full circles), the three M_{200} bins are represented by black, green and red circles, respectively (see caption of Figure 1). For comparison, the parameters for clusters Hercules and Abell 85 are overplotted (data taken from Agulli *et al.* 2016, 2017).

References

Agulli I., Aguerri J. A. L., Diaferio A., Dominguez Palmero L., Sánchez-Janssen R., 2017, *MNRAS*, 467, 4410

Agulli I., Aguerri J. a. L., Sánchez-Janssen R., Dalla Vecchia C., Diaferio A., Barrena R., Dominguez Palmero L., Yu H., 2016, *MNRAS*, 458, 1590

Bahé Y. M. *et al.*, 2017, *MNRAS*, 470, 4186

Barkhouse W. A., Yee H. K. C., López-Cruz O., 2007, *ApJ*, 671, 1471

Barnes D. J. *et al.*, 2017, *MNRAS*, 471, 1088

Blanton M. R., Lupton R. H., Schlegel D. J., Strauss M. A., Brinkmann J., Fukugita M., Loveday J., 2005, *ApJ*, 631, 208

Popesso P., Biviano A., Böhringer H., Romaniello M., 2006, *A&A*, 445, 29

Trayford J. W. *et al.*, 2015, *MNRAS*, 452, 2879

Vazdekis A., Koleva M., Ricciardelli E., Röck B., Falcón-Barroso J., 2016, *MNRAS*, 463, 3409

https://doi.org/10.1017/S1743921318006233 Published online by Cambridge University Press